Ultrarapid Generation of Femtoliter Microfluidic Droplets for Single-Molecule-Counting Immunoassays

Jung-uk Shim,[†,§,*] Rohan T. Ranasinghe,[†] Clive A. Smith,[†] Shehu M. Ibrahim,[†] Florian Hollfelder,[‡] Wilhelm T. S. Huck,[†,⊥] David Klenerman,[†] and Chris Abell[†]

[†]Department of Chemistry, University of Cambridge, Lensfield Road, Cambridge, U.K., CB2 1EW and [‡]Department of Biochemistry, University of Cambridge, Cambridge, U.K., CB2 1GA. [§]Present address: Biomedical Engineering, University of Glasgow, Glasgow, UK, G12 8LT. [⊥]Present address: Radboud University Nijmegen, Institute for Molecules and Materials, Heyendaalseweg 135, 6525 AJ Nijmegen, The Netherlands.

ABSTRACT We report a microfluidic droplet-based approach enabling the measurement of chemical reactions of individual enzyme molecules and its application to a single-molecule-counting immunoassay. A microfluidic device is used to generate and manipulate <10 fL droplets at rates of up to 1.3×10^6 per second, about 2 orders of magnitude faster than has previously been reported. The femtodroplets produced with this device can be used to encapsulate single biomolecular complexes tagged with a reporter enzyme; their small volume enables the fluorescent product of a single enzyme molecule to be detected within 10 min of on-chip incubation. Our prototype system is validated by detection of a biomarker for prostate cancer in buffer, down to a concentration of 46 fM. This work demonstrates a highly flexible and sensitive diagnostic platform that exploits extremely high-speed generation of monodisperse femtoliter droplets for the counting of individual analyte molecules.

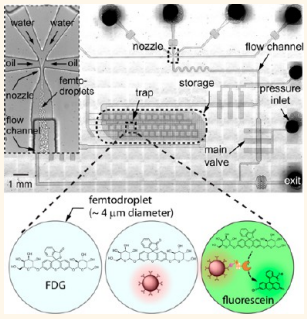

KEYWORDS: microfluidics · fast droplet generation · single-enzyme analysis · digital immunoassay

Water-in-oil droplets are emerging as a potentially powerful technology to quantitatively study compartmentalized reactions of single enzyme molecules and single cells because the concentration of reaction products or secreted molecules exceeds the detection threshold much more rapidly in small confined volumes[1] than in bulk solution. In order for the product resulting from turnover of a fluorogenic substrate by a single enzyme molecule to be detectable within a few minutes using epifluorescence microscopy, the volume of the reaction chamber has been reduced to less than 100 fL.[2−6] In this volume, a single molecule of enzyme has a concentration of ~17 pM, enabling catalyzed substrate turnover to dominate processes such as uncatalyzed hydrolysis, which in turn allows rapid accumulation and detection of the product. Due to their inherent scalability, droplet-based platforms could enable numerous single-molecule assays to be performed in parallel.

Ultrasmall droplets with volumes ranging from 0.5 fL to 2 pL have been used to detect the activity of single enzyme molecules, but the polydispersity of the emulsions used limited the precision and throughput of these studies.[7,8] In recent years, there has been tremendous progress in the development of microfluidics-based droplet platforms for the on-chip formation and manipulation of monodisperse droplets and the associated use of a range of fluorescence-based techniques for high-throughput and highly sensitive analysis of droplet contents.[1,9,10] Existing microfluidic devices normally generate highly monodisperse droplets at the pico- to nanoliter scale. In such volumes, several hours of enzymatic activity are required to turn over sufficient substrate for single enzyme molecule detection.[11] Most recently, Arayanarakool *et al.* reported the measurement of single-enzyme activity in femtoliter nanofluidic droplets, in which the droplet was incubated off-chip for several hours.[12] Furthermore, maximal droplet generation rates are in the 10 kHz range,[1,13] limiting high-throughput measurements of fast reactions.

The gold standard immunoassay, ELISA (enzyme-linked immunosorbent assay), enables the detection of biomarkers at concentrations above picomolar (10^{-12} M),[14]

* Address correspondence to junguk.shim@glasgow.ac.uk.

Received for review April 4, 2013 and accepted June 27, 2013.

Published online June 27, 2013
10.1021/nn401661d

but there remains an unmet clinical need for detection of biomarkers of neurodegenerative diseases and cancers that are present in biological fluids at concentrations in the range 10^{-12}–10^{-16} M;[15,16] the ability to detect single enzyme molecules provides a means to quantitate such low abundance markers. One promising approach uses the turnover of a fluorogenic substrate within well-arrays containing single enzyme molecules in an assay mixture or encased in a femtoliter water-in-oil droplet-array as the basis for ultrasensitive digital ELISAs.[17−20] However, the need for mechanical fabrication of femtoliter wells places inherent limits on the scalability and flexibility of ultrasensitive diagnostic assays, which could be overcome by carrying out experiments in microfluidic droplets.

We have developed a method based on a multilayered microfluidic device that enables the generation and manipulation of highly monodisperse femtoliter droplets at frequencies up to 1.3 MHz. This innovation allows us to measure the enzymatic activity of single enzyme molecules in a few minutes, a property that we have exploited to construct a bead-based ELISA for the detection of a low-abundance protein biomarker.

RESULTS AND DISCUSSION

Generation and Manipulation of Femtoliter-Volume Microfluidic Droplets. We have developed a microfluidic device for the controlled generation and manipulation of water-in-oil droplets with volumes of 5−50 femtoliters, which we call femtodroplets, at frequencies of >1 MHz (Figure 1a,e). Microfluidic droplets can be generated by shearing one fluid (water) by a second immiscible one (oil). In order to produce small water droplets at high frequencies, a large shear force and low surface tension at the oil−water interface are required. Large shear forces can be generated by either applying a high flow rate of oil or reducing the channel dimensions in order to increase the flow speed. However, high flow rates can lead to difficulties in device operation, and smaller channel dimensions produce high internal pressure, inversely proportional to the fourth power of the channel diameter.[21] In order to enhance the flow speed substantially during droplet formation without generating high internal pressure throughout the flow channel in the device, a flow-focusing nozzle was integrated into the design of our device. This strategy introduces a local constriction within a 300 μm section of the device, where the channel dimensions are reduced from 100 × 25 μm (width × depth) to 10 × 5 μm (Figure 1a,b). This nozzle enables the controlled generation of highly monodisperse aqueous droplets in fluorinated oil, previously mixed with a surfactant to decrease the interfacial tension and to prevent coalescence of droplets, at frequencies of 10^5–10^6 Hz (Figure 1e,f, Supporting Movies 1, 2).

We speculate that the femtodroplets produced by our device are formed by a tip-streaming mechanism in dripping mode, because an elongated water stream is visible at the nozzle orifice for the duration of the formation process (Supporting Movie 2) and the droplets formed are smaller than the width of the nozzle. The capillary number in our experiments (0.48−0.86) is also consistent with a previous report of droplet formation in the dripping regime.[22] It is known that the diameter of droplets formed by this mechanism can be 10-fold smaller than the orifice diameter, which would enable our device to generate femtoliter droplets. Also, the low viscosity of the fluorinated oil (∼1.2 cPs), compared to silicone oil (∼19 cPs) and mineral oil (∼123 cPs), enables us to overcome the inconveniently high hydrodynamic resistance in such a narrow flow-focusing nozzle, which is proportional to viscosity.[13,21,23,24]

The frequency of droplet formation was measured using a confocal optical setup, and the droplet volume calculated from the formation frequency and the flow rate of water. Using the current experimental setup, the maximally measurable frequency is 1.3 MHz, leading to a femtodroplet volume of 8.6 fL. However, very stable droplet generation at an oil flow rate of 480 μL/h was observed, where the droplet-generation frequency is expected to be 9.8 MHz according to the curve fit (Supporting Table 1), implying a femtodroplet volume of 1.1 fL (0.65 μm radius), although we cannot verify these rates experimentally using our current setup.

This droplet-generation frequency is about 2 orders of magnitude faster than previously reported.[1] We conclude that the locally narrow flow-focusing nozzle design and the low viscosity of the fluorinated oil are the key features that enable us to generate femtoliter droplets controllably at frequencies above a million hertz. The optical setup is being upgraded to measure higher droplet-formation frequencies, and further details will be reported separately. The femtodroplets formed using our device provide discrete reaction compartments that are small enough to enable the products of one molecule of enzyme to be detected within minutes by epifluorescence microscopy, but also large enough to be manipulated fluidically.

Once single enzyme molecules and the fluorogenic substrate have been encapsulated, it takes a few minutes to accumulate a measurable amount of fluorescent product by a typical reporter enzyme (β-galactosidase).[4,25] An area of 2 mm × 7 mm (length × width) was therefore integrated into the microfluidic device to store femtodroplets while the enzymatic reaction occurs (Figure 1b). This storage area is divided into 40 traps (300 × 300 μm), isolated by monolithic microfluidic valves (Figure 1b−d).[26−29] As the depth of the traps (5 μm) is comparable to the diameter of the femtodroplets, droplets stored in the microfluidic device are packed into a monolayer that allows fluorescence measurements of individual droplets using a simple epifluorescence microscope (Figure 2a). Trapping the femtodroplets in this way allows the activity of specific enzymes to be monitored continuously inside thousands

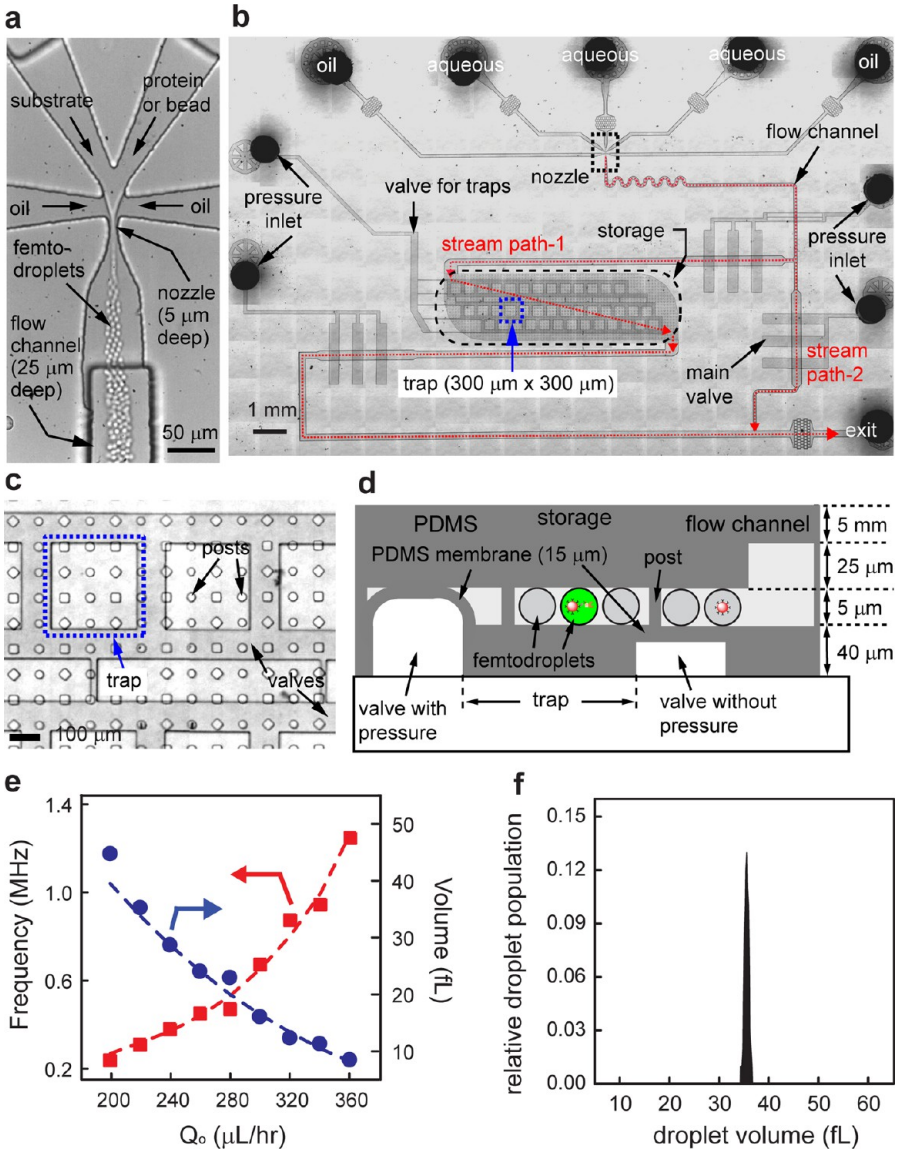

Figure 1. Features of the microfluidic device used for femtodroplet generation and manipulation. (a) Femtodroplet formation at the nozzle of the microfluidic device. Droplets with a typical volume of 32 fL are generated at a frequency of around 3.5×10^5 Hz. (b) Photograph of the whole multilayered PDMS device. The upper layer consists of the nozzle (10 μm wide $\times$ 5 μm deep), flow channels (100 μm wide $\times$ 25 μm deep), and storage compartments (2 mm wide $\times$ 7 mm long $\times$ 5 μm deep), with a capacity for $\sim 2 \times 10^5$ femtodroplets. The bottom layer houses the monolithic valves used to control droplet flow and isolate the traps. There are four injection holes for introduction of fluids into the device: the outer two for oil and the others for aqueous solutions. When the main valve is closed, the stream of femtodroplets is directed into the storage region (stream path 1). If this valve is opened, droplets flow out of the device by stream path 2 due to the lower flow resistance encountered. (c) Image of traps used for femtodroplet storage and isolation. The contents of the traps are manipulated by the action of networks of embedded monolithic valves in response to external pressure. (d) Vertical schematic of the storage structure. When pressure is applied, the thin PDMS membrane (15 μm thick) bends up to seal off the flow and traps the femtodroplets. (e) Generation frequency and volume of femtodroplets as a function of the oil flow rate (Q_o) at a constant water flow rate (Q_w) of 40 μL/h. In order to generate 32 fL droplets at a frequency of 350 kHz, we used oil and water flow rates of 230 and 40 μL/h, respectively. The dashed red line represents a fit of the experimental data to the equation $f = 3Q_w/\gamma^3 4\pi(a - Q_o/b)^3$, where f is the generation frequency, Q_w and Q_o are the respective flow rates of water and oil, $\gamma = 2$, and a and b are fitting parameters (see Supporting Table 1 for justification and discussion). The goodness of fit (r^2) is 0.99, returning fitting parameters of $a = 1.58$ and $b = 382$. The dashed blue line represents a fit to the same model, but with the frequency converted to droplet volume using the water flow rate, and is simply plotted to allow the reader to visualize both droplet volumes and generation frequencies. (f) Histogram of the droplet volumes obtained using flow rates of 40 μL/h of water and 220 μL/h of oil. The mean volume shown is 35.5 fL with a standard deviation of 0.66 fL.

of droplets simultaneously (Figure 2b). An embedded microfluidic valve is used to flush stored droplets out of the traps and reload freshly generated femtodroplets by application and release of external pressure (about 50 psi, Supporting Movie 3). This process takes only about 10 s due to the extremely high frequency of droplet generation and is therefore not rate-limiting for assay repetition.

Measurement of Reaction Time Courses of Individual Femtodroplet-Encapsulated Enzyme Molecules. As a first step in the

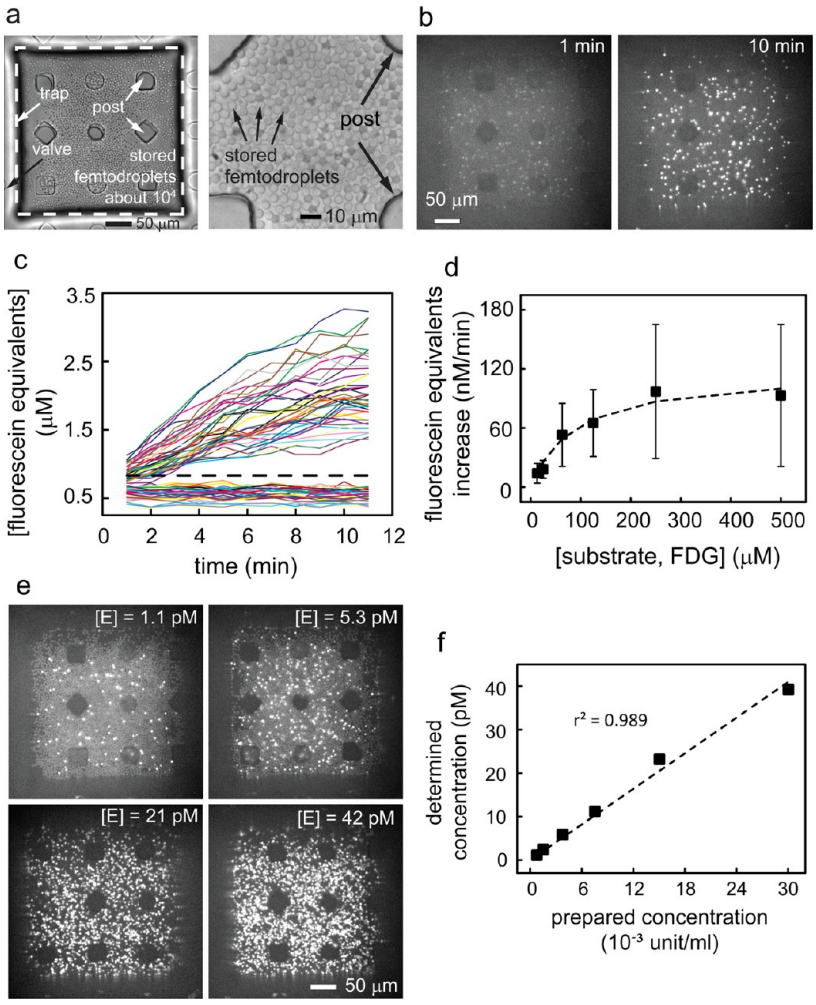

Figure 2. Measurement of the activity of single β-galactosidase molecules in femtodroplets. (a) Femtodroplets stored in a trap. The supporting posts maintain the shallow trap structure (5 μm deep). Droplets were packed in a monolayer in a trap (right). (b) Images showing green fluorescence resulting from hydrolysis of FDG (250 μM) by β-galactosidase (1.5×10^{-3} unit/mL, equivalent to 2.1 pM) in femtodroplets after 1 and 10 min. The bright spots represent femtodroplets enclosing a single enzyme molecule, in which fluorescent reaction products are generated. (c) Representative time traces of enzyme activity measured in femtodroplets that contain either one β-galactosidase molecule or none. The fluorescence intensity was measured every minute and converted to equivalent concentrations of fluorescein using a calibration curve after correcting for photobleaching (Supporting Figure 2); the concentration of fluorescein cannot be directly calculated due to the unknown contribution of the partially hydrolyzed product, fluorescein mono-β-D-galactopyranoside (FMG), to the observed fluorescence signal. The black dashed line represents a threshold, defined as three standard deviations above the mean of the background fluorescence after 10 min of incubation. The positive traces show a range of activities. (d) Kinetic saturation of fluorescence generation per single copy of β-galactosidase as a function of FDG concentration. The means and standard deviations (error bars) from a sample of ~150 femtodroplets enclosing a single copy of enzyme at each substrate concentration are plotted; the line connecting the data points was drawn merely to guide the eye. (e) Fluorescence micrographs of traps after 10 min incubation at various enzyme concentrations. The fraction of stored femtodroplets that show product formation varies in a concentration-dependent manner. (f) Plot of the prepared concentration (where one unit of enzyme hydrolyzes 1 μM of 2-nitrophenyl β-D-galactoside to 2-nitrophenol and D-galactose per minute at pH 7.3 at 37 °C) *vs* the experimentally determined molar concentration of β-galactosidase. The mean concentration determined from two replicates is plotted and fit with a linear function (dotted line).

development of our single-molecule ELISA, we optimized the substrate concentration and reaction time for the fluorescein di-β-D-galactopyranoside (FDG)/β-galactosidase reporter system in femtodroplets. β-Galactosidase (3.8×10^{-3} unit/mL, equivalent to 5 pM, yielding a probability of droplet occupancy of <0.1) was therefore encapsulated with FDG concentrations from 13 to 500 μM, and the fluorescence of ~150 enzyme-containing droplets monitored (Figure 2c,d, Supporting Movies 4−7). As enzymatic turnover starts at droplet generation, the initiation of the chemical reaction in each femtodroplet occurs essentially simultaneously (*i.e.*, within a second of each other) and so can be precisely monitored temporally. Inspection of the data in Figure 2d enabled us to establish the substrate concentration required to achieve kinetic saturation of fluorescence generation (250 μM), which was then used in all further experiments. Although FDG is a convenient and popular fluorogenic substrate for β-galactosidase, its diglysosylated structure results in a

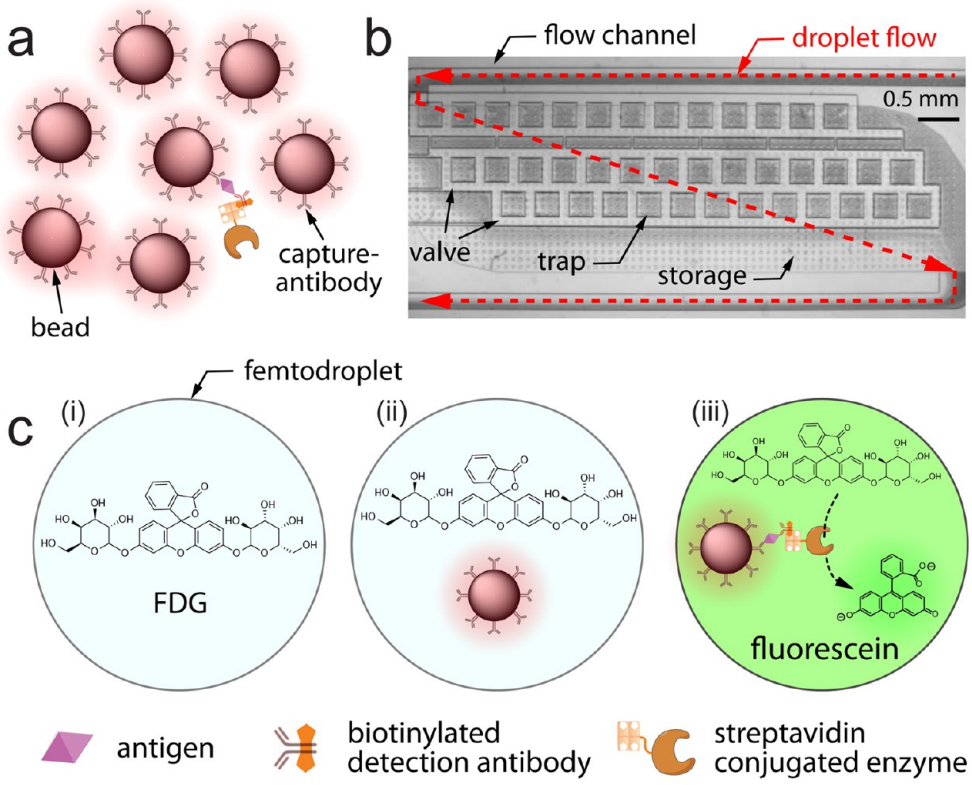

Figure 3. Schematic of single-molecule immunoassay using femtodroplets. (a) Binding of an antigen to antibody-coated beads; a single bead-captured target molecule is subsequently sandwiched by a biotinylated detection antibody and a streptavidin-β-galactosidase conjugate. (b) Beads with or without an immunocomplex are singly encapsulated in femtodroplets with a substrate (FDG) and subsequently on-chip incubated in traps to accumulate the fluorescent products of single-enzyme reporters. Each trap can enclose about 5×10^3 droplets, so the current storage capacity is about 2×10^5 droplets per chip. The stored droplets can be completely flushed out and reloaded in 10 s due to the extremely high-speed generation of droplets (Supporting Movie 3). (c) After the on-chip incubation, three populations of femtodroplets are observed: (i) droplets containing no bead, (ii) those containing a bead without immunocomplexes, and (iii) those containing a bead with an immunocomplex exhibiting a positive fluorescence signal due to the enzymatic activity of a single β-galactosidase reporter. The numerical ratio of (iii) to [(ii) + (iii)] yields the concentration of the target analyte. Thus, the larger the number of available droplets in a measurement, the better the detection sensitivity that can be accomplished in a given assay time.

sequential two-step hydrolysis mechanism, the kinetics of which have been the subject of some debate in the literature.[30,31] While this complication prohibits detailed kinetic analysis of our data, the similar saturation behavior found in bulk experiments (Supporting Figure 1) and the observed molecule-to-molecule variation of activity (CV = 64%)—in line with that reported by other laboratories[5,7,32]—demonstrate the viability of femtodroplets as a platform for single-molecule enzymology.

We then determined the time required for individual molecules of β-galactosidase encapsulated in 32 fL droplets to generate sufficient fluorescence signal to be detectable above the background using the optimal substrate concentration. The time course of fluorescence generation in approximately 5×10^3 femtodroplets containing 250 μM FDG was imaged at enzyme concentrations of up to 3×10^{-2} unit/mL (equivalent to about 40 pM), where the likelihood of enzyme occupancy in each droplet is <0.8 (Figure 2e, Supporting Movies 4−7). After incubation for 10 min, two populations of droplets were clearly visible (Figure 2b, Supporting Figure 3). The fraction of bright femtodroplets (Figure 2e)—with intensities separated from the mean fluorescence of the other dark droplet population by >3 SD (Figure 2c)—followed a Poisson distribution as a function of prepared enzyme concentration, as expected for product formation due to the activity of single molecules of β-galactosidase.[4,25] The linear relationship between the prepared and determined concentrations of β-galactosidase in Figure 2f confirmed that the activity observed in the bright femtodroplets was due to single enzyme molecules and that a 10-min incubation in femtodroplet-based digital ELISAs would enable counting of single analyte molecules with high statistical confidence.

Detection of a Cancer Biomarker Using a Femtodroplet Assay. The ability to sensitively detect β-galactosidase paves the way for ultrasensitive diagnostics using a bead-based ELISA to quantify very low concentrations (0.046−4.6 pM) of the biomarker prostate-specific antigen (PSA, molecular weight 30 kDa), reported by a single enzyme. A monoclonal antibody to the target protein was covalently coupled to 1 μm polystyrene

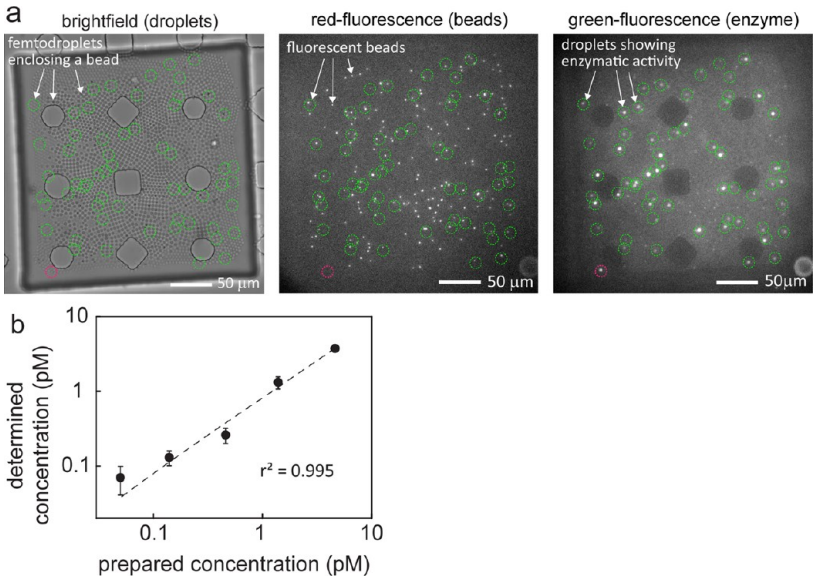

Figure 4. Detection of PSA using a femtodroplet ELISA. (a) Bright-field, red- and green-fluorescence images (left to right) of stored femtodroplets containing anti-PSA-coated beads (10 pM) and substrate (FDG, 250 μM) after a 10 min incubation period following immunoassay (in the presence of a 4.62 pM concentration of PSA) and subsequent encapsulation. Bright spots in the red-fluorescence micrograph result from beads conjugated with the capture antibody, while those in the green-fluorescence image are due to femtodroplets that contain an enzymatic reporter. The green circles in all images represent droplets that contain a bead and show enzymatic activity, while the red circles in the bottom left corner of each panel indicate a single femtodroplet that exhibits enzymatic activity but that does not contain a bead, indicating the presence of unbound enzyme in the droplet. (b) Plot of the concentrations of PSA measured by the droplet-based immunoassay *vs* the prepared concentration. The determined concentrations were calculated from a Poisson distribution function as described in Figure 2f, except that the fraction of beads encapsulated in droplets showing enzymatic activity (*e.g.*, the number ratio of green circles to fluorescent beads in part a) and the known bead concentration (10 pM) were used instead of the inactive fraction and volume of the femtodroplets. The means and standard deviations (error bars) from four replicate measurements are plotted and fit with a linear function (dotted line).

beads to enable capture in PBS buffer and subsequent detection of PSA in a sandwich complex containing a detector antibody specifically bound to a β-galactosidase reporter (Figure 3a). The capture beads exhibited red autofluorescence after covalent functionalization with monoclonal antibody, possibly due to the intrinsic fluorescence of immunoglobin.[33] This made it possible to count the number of beads by fluorescence imaging more easily than by using bright-field illumination, without interfering with the signal arising from enzyme-catalyzed hydrolysis of the substrate in the green part of the spectrum (Figure 4a).

At the end of each experiment, three different populations of femtodroplets were observed: (i) droplets containing no bead; (ii) droplets encapsulating a bead but without detectable enzymatic activity; and (iii) droplets containing a bead and a positive signal in green-fluorescence microscopy, corresponding to the presence of active enzyme conjugated to the target protein (Figure 3c). Since the concentration of PSA was lower than the bead concentration during anchoring of the target protein to the beads, Poisson statistics dictate that most beads capture either a single enzyme reporter or none.[4,25] As the bead concentration is known, the fraction of bead-containing femtodroplets that exhibit enzymatic turnover to the total number of beads can be used to calculate the concentration of PSA (Figure 4b, Supporting Table 3). The linear relationship obtained between the prepared and experimentally determined concentrations confirms that this approach can be used to quantify a low-abundance biomarker. The average capture efficiency in our assays is about 89%, which is slightly higher than that reported by Rissin *et al.* (>70%).[17] Failure to transduce all analyte molecules into bright femtodroplet signals may result from incomplete capture of PSA, dissociation of sandwich complexes during washing, or immobilization of inactive reporter enzymes; the higher bead concentration we used (10 pM *vs* 3.3 fM) might contribute to the enhanced transduction efficiency observed by increasing the fraction of captured antigen.

The lowest concentration of PSA assayed using our prototype system was 46 fM, or ~1.2 pg/mL, which led to an average of 12.0 bright femtodroplets (0.2% of bead-containing droplets) per experiment. This small number of events is subject to significant Poisson noise (theoretical and experimental CV = 28.8% and 30.4%, respectively), which limits quantification precision, but does permit detection with a high confidence level, provided the number of events observed in the absence of analyte (*e.g.*, resulting from nonspecific adsorption onto beads or carry-through of free reporter enzymes into the encapsulated mixture) is significantly lower. In the negative control—where the assay conditions were identical except that PSA was omitted—more than 3700 bead-containing droplets were analyzed,

none of which exhibited detectable reporter fluorescence after incubation. While this confirms that the detection of PSA at 46 fM is achieved with high statistical confidence, the limit of detection (LOD) cannot be accurately calculated without measuring a much larger number of negative control experiments, in order to obtain the mean and standard deviation of the number of bright droplets in the absence of analyte.[34] The lowest detected concentration in our assay is 1.2 pg/mL. This concentration is already comparable to the LOD for the most sensitive commercial bulk ELISAs (*e.g.*, ~3 pg/mL for Siemens' third-generation PSA test using the Immulite System), but considerably above that of state-of-the-art digital ELISAs.[17,18,35] This is because the sensitivity of our prototype system is limited by the number of femtodroplets measured per experiment. Currently ~20 000 droplets encapsulating ~1900 beads are analyzed per measurement, and the concentration of analyte required to generate an average of one fluorescent droplet in each experiment is 5.9 fM (given a capture efficiency of 89%). Assaying a 46 fM concentration of PSA is then expected to yield, on average, 8.0 bright femtodroplets per experiment (0.04% of droplets). However, if the entire storage capacity of the current prototype chip (200 000 droplets) was analyzed, the expected detection limit would fall to ~4.7 fM (0.12 pg/mL) without any modification to the assay or hardware.

CONCLUSION

In summary, this paper describes a microfluidic device that is able to generate and manipulate droplets with volumes of 5−50 fL at MHz frequencies. This femtoliter microfluidic droplet-based approach enables the measurement of the activity of a single copy of an enzyme and can be exploited to quantify very low abundance biomarkers by integrating a bead-based immunoassay with direct counting of individual enzyme molecules for developing a highly sensitive diagnostic test. The prototype system described is currently able to identify the presence of PSA in buffer at concentrations down to 46 fM (1.2 pg/mL), an improvement of nearly 2 orders of magnitude on standard ELISAs, whose detection limit is ~100 pg/mL. The method is conceptually similar to the digital ELISAs reported by Rissin *et al.*,[17] which employ solid femtoliter-sized wells that have been fabricated by mechanical methods.[18,35] The fluidic femtodroplet reaction chambers used in this study offer significant advantages due to the robustness and flexibility of the microfluidic circuit: extremely high-speed generation and on-chip manipulation of fast-flowing droplets, the ability to carry out replicate assays without replacing hardware, enabling a significant enhancement of the sampling size, ease of automation, and integration with other fluidic sample preparation modules; and the possibility of varying the size of the reactors at will.

The prospective clinical value of this femtodroplet diagnostic platform lies in its potential sensitivity and goes beyond current systems by its capacity for detection of multiple target proteins.[14,36] Further engineering of some of the features of this system will lead to an increase in sensitivity. Given the minimal nonspecific binding observed in the assay, it is very likely that subfemtomolar sensitivity could be achieved by concentrating the bead-captured biomarkers prior to encapsulation or by simply measuring a larger number of femtodroplets. Further improvements in the detection sensitivity could be achieved by increasing the throughput with which beads are analyzed. For example, establishing a high-throughput image acquisition system and a high-capacity microfluidic device would enable analysis of a larger number of beads in a given time. A complementary approach is to maximize the usage of droplets, since only 10% of droplets are occupied by beads under the current assay conditions, in order to ensure single-bead droplet occupancy during the Poissonian encapsulation process. This goal could be achieved by encapsulating multiple beads in each droplet; although this approach is incompatible with multiplexed assays, it would be useful for ultrasensitive single-analyte assays where the concentration of the target molecules is much lower than the bead concentration. Alternatively, Poisson-limited encapsulation could be bypassed altogether by evenly spacing the beads or concentrating them in the microfluidic device prior to droplet formation, to ensure that every droplet is occupied by a single bead.[37,38] Ultimately, the femtodroplet immunoassay used in this study should be able to display similar attomolar (10^{-18} M) limits of detection to those of state-of-the-art digital ELISAs, as the LOD is determined by assay-dependent parameters rather than the nature of the reaction chamber. Multiple protein markers could be detected by using different traps to carry out assays in parallel or by encoding antibodies with beads bearing distinct fluorescent signatures to enable multiplexing. While currently at an early stage, the microfluidic droplet-based platform we have developed has the potential to play a valuable role in the early identification and monitoring of diseases.[39]

METHODS

Microfluidic Device Fabrication. The microfluidic device was designed with AutoCAD (AutoDesk), and the corresponding photomasks were printed on transparencies (Micro Lithography Services) to enable fabrication of molds using a negative photoresist (SU8-2025, SU8-2005, Microchem). Microfluidic devices were made using two masters: the first for fabrication of the flow channels and storage chambers and the second for fabrication of the valve structures. A commercially available PDMS kit (Sylgard184, Dow Corning) containing a base and a

cross-linker was employed; the weight ratios (base:cross-linker) mixed for 5 mm and ~40 μm thickness PDMS slabs were 5:1 and 20:1, respectively. The mixed, degassed liquid PDMS (5:1 base:cross-linker ratio) was poured onto the first master and cured at 75 °C for 35 min. The resulting transparent, flexible silicone rubber was peeled off, and the fluid injection holes were punched through the slab. In order to fabricate the valve channels, a thin layer of liquid PDMS (base:cross-linker ratio of 20:1) was spin-coated onto the second master and the wafer cured at 85 °C for 5 min. After aligning the thick PDMS slab onto the thin PDMS layer, the device was baked for a further 30 min at 85 °C. The assembled PDMS slab was then peeled off the second master, and injection holes for application of pressure were punched. Finally, the multilayer device was sealed against an oxygen plasma-treated glass substrate, and Aquapel (Pittsburgh Glass Works) was applied to the flow-focusing nozzle to render it hydrophobic.

Device Operation. All fluids were injected into the microfluidic device by loading into individual syringes (Gastight, Hamilton) driven by syringe pumps (PHD 22/2000, Harvard Apparatus). Protein solutions or bead suspensions were mixed with a solution of substrate (500 μM fluorescein-di-β-D-galactopyranoside, FDG, Invitrogen) in PBS buffer (137 mM NaCl, 2.7 mM KCl, 8 mM Na_2HPO_4, and 2 mM KH_2PO_4, pH 7.4, Ambion) containing 0.1% v/v Tween-20 (Sigma) in the microfluidic device prior to droplet generation at the flow-focusing nozzle. Water droplets are formed in fluorinated oil (HFE-7500, Novec, 3M) previously mixed with a surfactant (5% w/w, Methods) to generate droplets stably and prevent their coalescence.

Fluorescence Image Acquisition and Analysis. Fluorescence images were obtained using an inverted microscope (IX71, Olympus) operated in epifluorescence mode using a mercury lamp (U-H100HG, Olympus) as an excitation source. The microfluidic devices were illuminated, and the emitted light was collected using the same objective (UPLSAPO 40 × 2, Olympus); excitation light was passed through a neutral density filter (25% transmission, Olympus) and only during image acquisition, in order to minimize photobleaching. Excitation light was spectrally filtered and separated from fluorescence emission using two mirror sets (excitation 475 ± 17 nm/emission 530 ± 22 nm, and excitation 559 ± 17 nm/emission 630 ± 35 nm, Thorlabs); green- and red-fluorescence micrographs were collected sequentially using a motorized filter cube (IX2-RFACA-1-5, Olympus) to alternate between the two colors. Images were acquired using an EMCCD camera (Xion+, Andor Technologies) with exposure times of 0.1 and 1 s for red and green fluorescence, respectively. Image analysis was performed using custom software written in LabView, which calculated the fluorescence intensity of femtodroplets by integrating the brightness of all the component pixels of each droplet.

Measurement of Femtodroplet-Generation Frequencies. A high-precision optical setup was used to measure the frequency of droplet formation. Briefly, the 488 nm beam of a diode laser (Spectra-Physics) was directed to the back port of an inverted microscope (Eclipse TE2000-U, Nikon), where it was reflected by a dichroic mirror and focused 2 μm above the cover slide into the flow-focusing nozzle of the microfluidic device, using an oil-immersion objective (Apochromat 60×, NA 1.40, Nikon). Fluorescence was collected by the same objective and imaged onto a 70 μm pinhole (Melles Griot) to exclude out-of-focus light, forming a confocal detection volume of ~0.1 fL. Green fluorescence was filtered by a pair of long-pass and band-pass filters (540ALP and 535AF45, Omega Optical Filters) before being focused onto an avalanche photodiode (APD, SPCM-14, PerkinElmer). The readout from the APD was coupled to a PC-implemented multichannel scalar (MCS) card and analyzed with custom-written software. Fluorescence was recorded as raw photon counts over a typical window of 50 ns. Femtodroplets were generated as described above, using 0.2 μM fluorescein in PBS buffer containing 0.1% v/v Tween-20 as the aqueous phase, and the frequency of droplet formation was calculated from the separation of the resulting fluorescence bursts in the MCS output. A fast camera (MIRO4, Vision Research) was used to visually confirm droplet generation and enable alignment of the confocal spot within the flow-focusing nozzle, while an extremely high speed camera (up to 1.0 Mfps, V1610, Vision Research) was used to capture movies of droplet generation (Supporting Movie 2).

Surfactant Synthesis. Methanol (5 mL, Fisher) was added to a stirred solution of Krytox 157 FSL (15.3 g, 6.1 mmol) in HFE-7500 (15 mL, Novec, 3M) under nitrogen at room temperature, and the mixture stirred for 16 h. The solution was evaporated to dryness, and IR analysis (1775.8 cm^{-1}) indicated little or no conversion to the methyl ester. The resulting oil was dissolved in HFE-7100 (15 mL, Novec, 3M), and a solution of *O*, *O'*-bis(2-aminopropyl)polypropylene glycol-*block*-polyethylene glycol-*block*-polypropylene glycol (1.827 g, Jeffamine ED-600, Sigma) in methanol (5 mL) was added *via* syringe and stirred under nitrogen for 96 h at room temperature. The solution was evaporated to dryness and placed under high vacuum. In order to remove any diblock surfactant or free amine, the oil was dissolved in HFE-7100 (35.0 mL) and stirred with 3-(isocyanato)-propyl-functionalized silica gel (1 g, 1.20 mmol/g, 200–400 mesh, Sigma) under nitrogen for 5 h at room temperature. The solution was filtered through Celite, which was then washed three times with HFE-7100 (15 mL). This solution was filtered through a syringe filter (33 mm × 0.22 μm, Millex) and evaporated to dryness to give Krytox 157 FSL Jeffamine ED-600 disalt surfactant as a colorless oil (14.4 g, 83.9%). IR: 1699.7 cm^{-1}.

Bulk Enzyme Measurements. Bulk enzyme experiments were performed on a FLASHScan microtiter plate reader (Analytik Jena). A final enzyme concentration of 10 μg/mL of (after dilution with substrate solution) was used at eight substrate concentrations (FDG, 12.5, 25, 50, 100, 200, 400, 600, 800 μM). The rate of fluorescence generation was converted to fluorescein equivalent units at each substrate concentration by comparison with a fluorescein standard curve.

Measurement of Activities of Single Enzyme Molecules. β-Galactosidase (Roche, at concentrations of 0.75, 1.5, 3.75, 7.5, 15, and 30 × 10^{-3} unit/mL) was prepared in PBS buffer containing 0.1% v/v Tween-20 and loaded into a syringe (Hamilton, Gastight, 250 μL), and FDG (500 μM), prepared in PBS buffer containing 0.1% v/v Tween-20, was loaded into the second identical syringe; both solutions were injected into the microfluidic device in a 1:1 volume ratio and emulsified with fluorinated oil premixed with surfactant (5% w/w). After trapping the femtodroplets in the device, the fluorescence intensity of stored droplets was measured every minute and converted to fluorescein equivalents using a calibration curve after correcting for photobleaching (SI Figure 1). Droplets containing reporter enzymes were identified according to an AND thresholding procedure. Only femtodroplets whose intensity exceeded the mean of negative control droplets plus three standard deviations and that exhibited significant fluorescence increase during incubation were classified as "positive". The latter criterion enabled us to exclude droplets with high fluorescence intensities due to the presence of dust or other autofluorescent contaminants.

In order to measure the enzyme activity as a function of substrate concentration, β-galactosidase (3.8 × 10^{-3} units/mL, equivalent to about 5 pM) and FDG (13, 25, 63, 125, 250, or 500 μM) were prepared in PBS buffer containing 0.1% v/v Tween-20 and loaded into syringes (Hamilton, Gastight, 250 μL), respectively. The droplets were formed and the product formation was measured as described above.

Preparation of Beads Conjugated with Capture Antibody, Capture of the Target Protein Sandwiched with Detection Antibody, and Enzymatic Reporters. Capture beads were prepared by covalently coupling amino-functionalized polystyrene microspheres (1 μm diameter, Polysciences) to anti-PSA antibody (R&D Systems) *via* a glutaraldehyde cross-linker, introduced using a commercial coupling kit (Polysciences) according to the manufacturer's instructions.

Antibody-functionalized capture beads (10 pM) were mixed with PSA (M_w 30 kDa, R&D Systems, at concentrations of 0.046, 0.14, 0.46, 1.39, and 4.62 pM) in a final volume of 200 μL of PBS buffer containing 0.1% v/v Tween-20 and incubated for 2 h at room temperature. The beads were then recovered by centrifugation (12100*g* for 6 min), the supernatant was discarded, and the particles were resuspended and sonicated for 3 min in PBS

buffer containing 0.1% v/v Tween-20 (200 μL). This washing process was repeated twice before resuspension in a solution of biotinylated polyclonal anti-PSA (R&D Systems, 0.9 nM) in PBS buffer containing 0.1% v/v Tween-20 (200 μL) and incubation for 1 h at room temperature. The beads were then recovered by centrifugation (12100*g* for 6 min), the supernatant was discarded, and the particles were resuspended and sonicated for 3 min in PBS buffer containing 0.1% v/v Tween-20 (200 μL). This washing process was repeated twice before resuspension in a solution of streptavidin-conjugated β-galactosidase (Invitrogen, 25 pM) in PBS buffer containing 0.1% v/v Tween-20 (200 μL) and incubation for 1 h. The beads were then recovered by centrifugation (12100*g* for 6 min), the supernatant was discarded, and the particles were resuspended and sonicated for 3 min in PBS buffer containing 0.1% v/v Tween-20 (200 μL). This washing process was repeated six times before injection into the microfluidic device.

Conflict of Interest: The authors declare no competing financial interest.

Acknowledgment. We acknowledge financial support from the Engineering and Physical Sciences Research Council and the European Commission (TheraEDGE Network Contract FP7-216027). J-u.S. thanks the EU for a Marie-Curie fellowship and the Isaac Newton Trust for a fellowship. F.H. is an ERC Starting Investigator. The authors thank N. Tokuriki for a critical suggestion, M. Fischlechner and X. Li for helpful discussions, X. Xu for the bulk enzyme measurements, A. Zhukov for homemade software, P. Jönsson for a critical reading of the manuscript, and Vision Research for the loan of an ultra-high-speed camera. A provisional application for a GB patent on this approach has been filed.

Supporting Information Available: Movies and supporting experimental and theoretical data for this article are available free of charge *via* the Internet at http://pubs.acs.org.

REFERENCES AND NOTES

1. Theberge, A. B.; Courtois, F.; Schaerli, Y.; Fischlechner, M.; Abell, C.; Hollfelder, F.; Huck, W. T. S. Microdroplets in Microfluidics: An Evolving Platform for Discoveries in Chemistry and Biology. *Angew. Chem., Int. Ed.* **2010**, *49*, 5846–5868.
2. Chiu, D. T.; Wilson, C. F.; Ryttsen, F.; Stromberg, A.; Farre, C.; Karlsson, A.; Nordholm, S.; Gaggar, A.; Modi, B. P.; Moscho, A.; *et al*. Chemical Transformations in Individual Ultrasmall Biomimetic Containers. *Science* **1999**, *283*, 1892–1895.
3. Comellas-Aragones, M.; Engelkamp, H.; Claessen, V. I.; Sommerdijk, N.; Rowan, A. E.; Christianen, P. C. M.; Maan, J. C.; Verduin, B. J. M.; Cornelissen, J.; Nolte, R. J. M. A Virus-Based Single-Enzyme Nanoreactor. *Nat. Nanotechnol.* **2007**, *2*, 635–639.
4. Rondelez, Y.; Tresset, G.; Tabata, K. V.; Arata, H.; Fujita, H.; Takeuchi, S.; Noji, H. Microfabricated Arrays of Femtoliter Chambers Allow Single Molecule Enzymology. *Nat. Biotechnol.* **2005**, *23*, 361–365.
5. Rissin, D. M.; Gorris, H. H.; Walt, D. R. Distinct and Long-Lived Activity States of Single Enzyme Molecules. *J. Am. Chem. Soc.* **2008**, *130*, 5349–5353.
6. Cai, L.; Friedman, N.; Xie, X. S. Stochastic Protein Expression in Individual Cells at the Single Molecule Level. *Nature* **2006**, *440*, 358–362.
7. Rotman, B. Measurement of Activity of Single Molecules of Beta-D-Galactosidase. *Proc. Natl. Acad. Sci. U.S.A.* **1961**, *47*, 1981–1991.
8. Lee, A. I.; Brody, J. P. Single-Molecule Enzymology of Chymotrypsin Using Water-in-Oil Emulsion. *Biophys. J.* **2005**, *88*, 4303–4311.
9. Chiu, D. T.; Lorenz, R. M.; Jeffries, G. D. M. Droplets for Ultrasmall-Volume Analysis. *Anal. Chem.* **2009**, *81*, 5111–5118.
10. Guo, M. T.; Rotem, A.; Heyman, J. A.; Weitz, D. A. Droplet Microfluidics for High-Throughput Biological Assays. *Lab Chip* **2012**, *12*, 2146–2155.
11. Joensson, H. N.; Samuels, M. L.; Brouzes, E. R.; Medkova, M.; Uhlen, M.; Link, D. R.; Andersson-Svahn, H. Detection and Analysis of Low-Abundance Cell-Surface Biomarkers Using Enzymatic Amplification in Microfluidic Droplets. *Angew. Chem., Int. Ed.* **2009**, *48*, 2518–2521.
12. Arayanarakool, R.; Shui, L.; Kengen, S. W. M.; Van Den Berg, A.; Eijkel, J. C. T. Single-Enzyme Analysis in a Droplet-Based Micro- and Nanofluidic System. *Lab Chip* **2013**, *13*, 1955–1962.
13. Holtze, C.; Rowat, A. C.; Agresti, J. J.; Hutchison, J. B.; Angile, F. E.; Schmitz, C. H. J.; Koster, S.; Duan, H.; Humphry, K. J.; Scanga, R. A.; *et al*. Biocompatible Surfactants for Water-in-Fluorocarbon Emulsions. *Lab Chip* **2008**, *8*, 1632–1639.
14. Giljohann, D. A.; Mirkin, C. A. Drivers of Biodiagnostic Development. *Nature* **2009**, *462*, 461–464.
15. Holtzman, D. M.; Morris, J. C.; Goate, A. M. Alzheimer's Disease: The Challenge of the Second Century. *Sci. Transl. Med.* **2011**, *3*, 77sr1.
16. Hanash, S. M.; Baik, C. S.; Kallioniemi, O. Emerging Molecular Biomarkers-Blood-Based Strategies to Detect and Monitor Cancer. *Nat. Rev. Clin. Oncol.* **2011**, *8*, 142–150.
17. Rissin, D. M.; Kan, C. W.; Campbell, T. G.; Howes, S. C.; Fournier, D. R.; Song, L.; Piech, T.; Patel, P. P.; Chang, L.; Rivnak, A. J.; *et al*. Single-Molecule Enzyme-Linked Immunosorbent Assay Detects Serum Proteins at Subfemtomolar Concentrations. *Nat. Biotechnol.* **2010**, *28*, 595–599.
18. Kan, C. W.; Rivnak, A. J.; Campbell, T. G.; Piech, T.; Rissin, D. M.; Mosl, M.; Peterca, A.; Niederberger, H. P.; Minnehan, K. A.; Patel, P. P.; *et al*. Isolation and Detection of Single Molecules on Paramagnetic Beads Using Sequential Fluid Flows in Microfabricated Polymer Array Assemblies. *Lab Chip* **2012**, *12*, 977–985.
19. Kim, S. H.; Iino, R.; Iwai, S.; Araki, S.; Sakakihara, S.; Noji, H. Large-Scale Femtoliter Droplet Array for Digital Counting of Single Biomolecules. *Lab Chip* **2012**, *12*, 4986–4991.
20. Witters, D.; Knez, K.; Ceyssens, F.; Puers, R.; Lammertyn, J. Digital Microfluidics-Enabled Single-Molecule Detection by Printing and Sealing Single Magnetic Beads in Femtoliter Droplets. *Lab Chip* **2013**, *13*, 2047–2054.
21. Beebe, D. J.; Mensing, G. A.; Walker, G. M. Physics and Applications of Microfluidics in Biology. *Annu. Rev. Biomed. Eng.* **2002**, *4*, 261–286.
22. Anna, S. L.; Mayer, H. C. Microscale Tipstreaming in a Microfluidic Flow Focusing Device. *Phys. Fluids* **2006**, *18*, 121512.
23. Jeong, W. C.; Lim, J. M.; Choi, J. H.; Kim, J. H.; Lee, Y. J.; Kim, S. H.; Lee, G.; Kim, J. D.; Yi, G. R.; Yang, S. M. Controlled Generation of Submicron Emulsion Droplets *via* Highly Stable Tip-Streaming Mode in Microfluidic Devices. *Lab Chip* **2012**, *12*, 1446–1453.
24. Cristini, V.; Tan, Y. C. Theory and Numerical Simulation of Droplet Dynamics in Complex Flows - A Review. *Lab Chip* **2004**, *4*, 257–264.
25. Rissin, D. M.; Walt, D. R. Digital Concentration Readout of Single Enzyme Molecules Using Femtoliter Arrays and Poisson Statistics. *Nano Lett.* **2006**, *6*, 520–523.
26. Unger, M. A.; Chou, H. P.; Thorsen, T.; Scherer, A.; Quake, S. R. Monolithic Microfabricated Valves and Pumps by Multilayer Soft Lithography. *Science* **2000**, *288*, 113–116.
27. Shim, J. U.; Cristobal, G.; Link, D. R.; Thorsen, T.; Jia, Y. W.; Piattelli, K.; Fraden, S. Control and Measurement of the Phase Behavior of Aqueous Solutions Using Microfluidics. *J. Am. Chem. Soc.* **2007**, *129*, 8825–8835.
28. Shim, J. U.; Patil, S. N.; Hodgkinson, J. T.; Bowden, S. D.; Spring, D. R.; Welch, M.; Huck, W. T. S.; Hollfelder, F.; Abell, C. Controlling the Contents of Microdroplets by Exploiting the Permeability of PDMS. *Lab Chip* **2011**, *11*, 1132–1137.
29. Shim, J. U.; Olguin, L. F.; Whyte, G.; Scott, D.; Babtie, A.; Abell, C.; Huck, W. T. S.; Hollfelder, F. Simultaneous Determination of Gene Expression and Enzymatic Activity in Individual Bacterial Cells in Microdroplet Compartments. *J. Am. Chem. Soc.* **2009**, *131*, 15251–15256.
30. Fiedler, F.; Hinz, H. No Intermediate Channeling in Stepwise Hydrolysis of Fluorescein Di-Beta-D-Galactoside by Beta-Galactosidase. *Eur. J. Biochem.* **1994**, *222*, 75–81.
31. Hofmann, J.; Sernetz, M. A Kinetic-Study on the Enzymatic-Hydrolysis of Fluoresceindiacetate and Fluorescein-Di-Beta-D-Galactopyranoside. *Anal. Biochem.* **1983**, *131*, 180–186.

32. Lu, H. P.; Xun, L. Y.; Xie, X. S. Single-Molecule Enzymatic Dynamics. *Science* **1998**, *282*, 1877–1882.
33. Eftink, M. R. Fluorescence Techniques for Studying Protein-Structure. *Methods Biochem. Anal.* **1991**, *35*, 127–205.
34. Armbruster, D. A.; Pry, T. Limit of Blank, Limit of Detection and Limit of Quantitation. *Clin. Biochem. Rev.* **2008**, *29* (Suppl 1), S49−52.
35. Zhang, H. B.; Nie, S.; Etson, C. M.; Wang, R. M.; Walt, D. R. Oil-Sealed Femtoliter Fiber-Optic Arrays for Single Molecule Analysis. *Lab Chip* **2012**, *12*, 2229–2239.
36. Buchen, L. Missing the Mark. *Nature* **2011**, *471*, 428–432.
37. Edd, J. F.; Di Carlo, D.; Humphry, K. J.; Koster, S.; Irimia, D.; Weitz, D. A.; Toner, M. Controlled Encapsulation of Single-Cells into Monodisperse Picolitre Drops. *Lab Chip* **2008**, *8*, 1262–1264.
38. Abate, A. R.; Chen, C. H.; Agresti, J. J.; Weitz, D. A. Beating Poisson Encapsulation Statistics Using Close-Packed Ordering. *Lab Chip* **2009**, *9*, 2628–2631.
39. Whitesides, G. M. The Origins and the Future of Microfluidics. *Nature* **2006**, *442*, 368–373.